



# Comparison of Radial and Halbach Array PMLSM by Employing 2-D Electromagnetic Finite Element Analysis

Hassan Moradi Cheshmeh Beigi<sup>1,\*</sup> and Allahdad Khanmohamadian<sup>1</sup>

<sup>1</sup>Electrical Engineering Department, Faculty of Engineering, Razi University, Kermanshah, Iran.

\*Corresponding Author's Information: ha.moradi@razi.ac.ir

## ARTICLE INFO

### ARTICLE HISTORY:

Received 03 September 2016  
Revised 25 November 2016  
Accepted 26 November 2016

### KEYWORDS:

EMALS  
FEM  
Radial Array  
Halbach Shaped magnets  
PMLSM

## ABSTRACT

The replacement of steam catapults with electromagnetic ones is becoming an overwhelming trend in aircraft launch systems. The Electromagnetic Aircraft Launch System (EMALS) offers significant benefits to the aircraft, ship, personnel, and operational capabilities. EMALS has many advantages such as high thrust, good controllability, etc. As a launching motor, a double-sided plate Permanent Magnet Linear Synchronous Motor (PMLSM) can provide high instantaneous thrust. This paper compares two PM mover with quasi-Halbach array topology and radial topology for PMLSM application. A detailed analytical modeling based on Maxwell equations is presented for analysis and design of PMLSM with Halbach array. Finally, 2-D non-linear time-stepping transient finite element method is employed to demonstrate validity of the theoretical analysis and parametric search. Using FEA, the effects of the parameters on the thrust amplitude are analyzed. Finally, A design optimization method is applied to PMLSM with Halbach array. The obtained results form 2-D FEM show the increase of thrust force and flux density distribution in the air gap.

## 1. INTRODUCTION

The USA Navy is presently pursuing electromagnetic launch technology to replace the existing steam catapults on current and future aircraft carriers. The steam catapults are large, heavy, and operate without feedback control. They impart large transient loads to the airframe and are difficult and time-consuming to maintain [1]. The steam catapult is also approaching its operational limit with the present complement of naval aircraft. The inexorable trend towards heavier, faster aircraft will soon result in launch energy requirements that exceed the capability of the steam catapult. An electromagnetic launch system offers higher launch energy capability, as well as substantial improvements in areas other than performance. These include reduced weight, volume, and maintenance; and increased controllability, availability, reliability, and efficiency [2]. In this paper, the linear motor part of EMALS is further discussed. The linear motor for

electromagnetic launch generally requires high voltage, high current, high and constant thrust. The variation range of transient velocity for mover is very large, and the terminal velocity can reach several tens meters per second. All those special conditions require high thrust output and energy efficiency for permanent-magnet linear synchronous motor (PMLSM). Therefore, the investigation of structural and electrical parameters effects is necessary to promote performance of PMLSM design [3]. A PMLSM utilized in EMALS is chosen based on several key advantages, including high-power density, strength of the field, and efficiency. In addition, since permanent-magnet requires no external excitation to produce a magnetic field, no brushes, slip rings, or other connections to the moving translator are necessary [4]. The PMLSM with Halbach array exhibits an essentially sinusoidal air-gap field distribution and a sinusoidal Back-EMF waveform, as well as negligible

cogging force, without employing skew or distributed winding [5]. In the recent years, PMLSM has been proven to provide the best all-around performance for EMALS applications in comparison with induction-type motor because of its high force, and high efficiency [6]. The double-sided plate PMLSM has been paid more attention for the EMALS. For the double-sided plate motor, the two-sided normal forces counteract each other, so it can avoid the impact of a unilateral magnetic pull [7].

## 2. FIELD DISTRIBUTION DUE TO PERMANENT-MAGNET SOURCE

In order to establish analytical solutions for the magnetic field distribution in the foregoing machine topology, the following assumptions are made:

- The length of machine is extended to infinity.
- The permeability of iron core is infinite.
- The permeability of the permanent-magnet material is equal to the permeability of the free space.

Consequently, the magnetic field analysis is confined to two regions, the airspace/winding and permanent-magnet region. Figure 1 shows the simplified model of the machine.

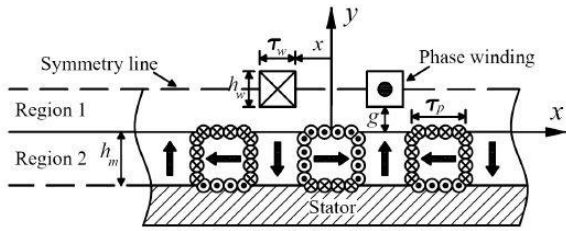


Figure 1: Simplified model of the machine and the equivalent magnetization current distribution.

Therefore, the governing field equations, in terms of magnetic vector potential lead to Laplace and Poisson equations as follows [10]:

$$\begin{cases} \nabla^2 A_1 = 0 & \text{in region 1} \\ \nabla^2 A_2 = -\mu_0 J_M & \text{in region 2} \end{cases} \quad (1)$$

where  $J_M = \nabla \times \mathbf{M}$  and  $\mathbf{M}$  is magnetization vector of PMLSM with Halbach array and is given by:

$$\mathbf{M} = M_x \mathbf{a}_x + M_y \mathbf{a}_y \quad (2)$$

Where  $M_x$  and  $M_y$  denote the components of  $\mathbf{M}$  in  $x$  and  $y$  directions, respectively, and may be expressed as Fourier series:

$$M_x = \sum_{n=1,3,\dots}^{\infty} P_n \sin\left(\frac{m_n \tau_p}{2}\right) \cos(m_n x) \quad (3)$$

$$M_y = \sum_{n=1,3,\dots}^{\infty} P_n \cos\left(\frac{m_n \tau_p}{2}\right) \sin(m_n x) \quad (4)$$

where  $P_n = \frac{4B_r}{n\pi\mu_0}$  and  $m_n = \frac{n\pi}{\tau}$ . The boundary conditions to be satisfied in (1) are:

$$\left\{ \begin{array}{l} H_{2x}|_{y=0} - H_{1x}|_{y=0} = M_x; \quad H_{2x}|_{y=-l_m} = M_x \\ H_{1x}|_{y=g+l_w/2} = 0; \quad H_{2x}|_{y=-l_m} = M_x \end{array} \right\} \quad (5)$$

By solving (1), the tangential and normal components ( $B_x$  and  $B_y$ ) of the flux density produced by the permanent-magnets in the air gap are provided from the curl of  $A_2$  and are given by:

$$B_{1x}(x, y) = - \sum_{n=1,3,\dots}^{\infty} m_n \left( \begin{array}{c} a_{1n} \sinh(m_n x) \\ + \\ b_{1n} \cosh(m_n x) \end{array} \right) \cos(m_n x) \quad (6)$$

$$B_{1y}(x, y) = \sum_{n=1,3,\dots}^{\infty} m_n \left( \begin{array}{c} a_{1n} \cosh(m_n x) \\ + \\ b_{1n} \sinh(m_n x) \end{array} \right) \sin(m_n x) \quad (7)$$

where  $a_{1n}$  and  $b_{1n}$  are as follows:

$$a_{1n} = \left( \frac{P_n \mu_0}{2m_n e^{2m_n(h_m+g+l_w)} - 2m_n} \right) \left[ \begin{array}{l} \left( \sin\left(\frac{m_n \tau_p}{2}\right) + \cos\left(\frac{m_n \tau_p}{2}\right) \right) e^{2m_n h_m} - \\ 2 \sin\left(\frac{m_n \tau_p}{2}\right) e^{m_n h_m} + \sin\left(\frac{m_n \tau_p}{2}\right) - \\ \cos\left(\frac{m_n \tau_p}{2}\right) \end{array} \right] \quad (8)$$

$$b_{1n} = e^{2m_n(g+l_w)} \cdot a_{1n}$$

## 3. FIELD LORENTZ FORCE

The thrust force exerted on the armature, resulting from the interaction between the winding current and the permanent-magnet field, is given by:

$$\mathbf{F} = \int_V \mathbf{J} \times \mathbf{B} dV \quad (9)$$

Assuming that each coil side on the armature occupies areas bounded by:

$$\left\{ \begin{array}{l} x_1 = x - \frac{\tau_w}{2}, x_2 = x + \frac{\tau_w}{2} \\ y_1 = g, y_2 = g + h_w \end{array} \right\} \quad (10)$$

The total thrust force exerted on the one coil side may be obtained from the following integration [11]:

$$F = 2 \int_{x-\tau_w/2}^{x+\tau_w/2} \int_g^{g+h_w/2} (LJB_{1y}) dx dy \quad (11)$$

which may be written as:

$$F = \sum_{n=1,3,\dots}^{\infty} K_n \sin(m_n x) \quad (12)$$

where  $K_n$  is given by:

$$K_n = 4LJp_f k_{wm} \sin\left(\frac{m_n \tau_w}{2}\right) [a_{1n} \sin h(m_n x) + b_{1n} \cosh(m_n x)] dy \quad (13)$$

Therefore, the total force  $F_{1ph}$  exerted on a phase winding comprising a number of series connected coils, is obtained as:

$$F_{1ph} = \sum_{n=1,3,\dots}^{\infty} F_n \cos m_n \left(x - \frac{\tau_{wp}}{2}\right) \quad (14)$$

where  $F_n$  is defined as thrust constant of the  $n^{th}$  harmonic, and is given by:

$$F_n = 2PK_n \sin\left(\frac{m_n \tau_{wp}}{2}\right) \quad (15)$$

Referring to (15), the normalized total thrust ripples are given by:

$$TTR = \frac{\sqrt{\sum_{n=5,7,11,13,\dots}^{\infty} F_n^2}}{F_1} \quad (16)$$

#### 4. NUMERICAL ANALYSIS OF MAGNETIC FIELD FOR PMLSM WITH RADIAL ARRAY AND HALBACH ARRAY STRUCTURE

Due to the complex geometry, non-linear property and magnetic saturation effect, the design procedure and accuracy evaluation of understudy configuration become more complicated.

To evaluate the accuracy of design procedure and performance of PMLSM with radial array and Halbach array, two dimensional finite element analysis is performed. An accurate flux distribution for different mover position is investigated.

The relative movement is taken into account in the FEM by using time-stepping transient analysis and Lagrange multiplier method [12].

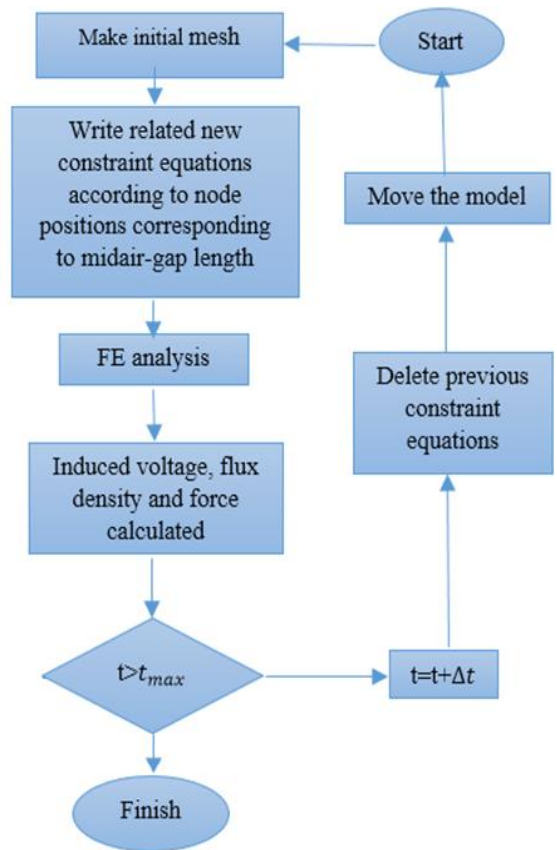


Figure 2: Flowchart of FEM analysis.

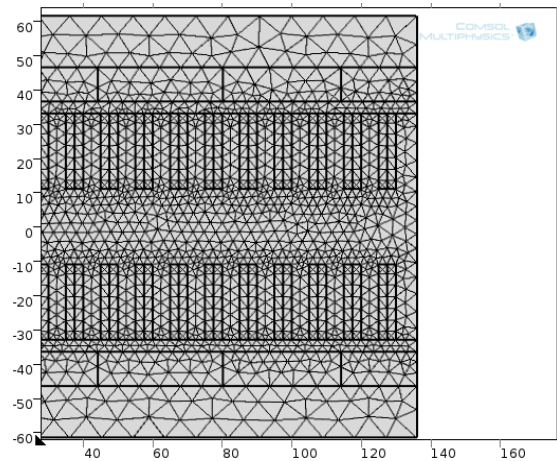


Figure 3: The triangular meshed model of PMLSM by FEA.

A flowchart of the FEM is shown in Figure 2. The PMLSM 2-D FEM model consists of 10000 elements and 30000 meshes. So, a FE analysis has been used to build and solve non-linear magnetic models of the proposed PMLSM.

One side of the PMLSM cross section is shown in Figure 3. It can be seen that the magnets, drive coil and tooth are relative intensive so as to ensure the accuracy of simulation.

The magnetic-flux-line for PMLSM is shown in Figure 4. It can be seen that the magnetic-flux-line in PMC-PMLSM is parallel and the magnetic circuit structure is complex and uniform with low flux leakage.

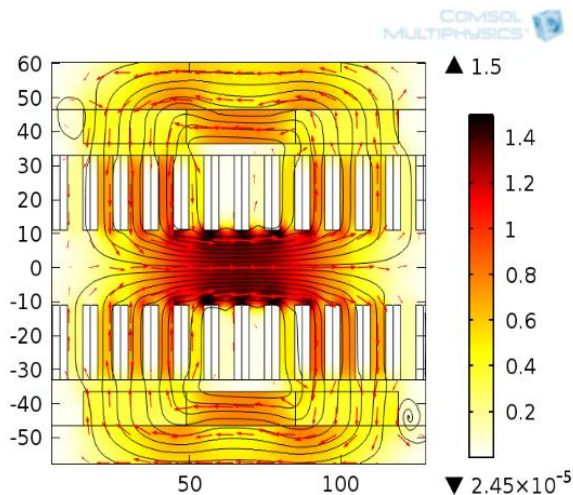


Figure 4: The flux leakage distribution for PMLSM.

### 5. RADIAL AND HALBACH ARRAY PMLSM TOPOLOGY

In this paper, two PM mover with quasi-Halbach array topology and radial topology for PMLSM application are compared.

Figure 5 shows a Topology PMLSM (a) radial array, and (b) quasi-Halbach array, both motors having identical stators.

The structural model of PMLSM is composed of permanent magnets (PMs) in secondary and coil winding with slotted stator in long primary. A Radial array, which is a special case of PM motors, is less used for PMLSM applications because of its high ripple force production.

In order to reduce thrust ripple and increase flux density, the optimized quasi-Halbach magnetized topology can be applied to the PMLSM [8]. Quasi-Halbach topology has a self-shielding property and higher flux density than Radial topology. Due to the different magnetization direction of permanent magnet on two sides, there are two types of magnetic circuit: parallel magnetic circuit (PMC) and serial magnetic circuit (SMC).

PMC- PMLSM has a moving-magnet type secondary, which composed of double-sided permanent magnets arranged by N face N direction, while the SMC-PMLSM composed of double-sided permanent magnets arranged by N face S direction.

Usually, the PMC- PMLSM is adopted, because, it can generate a larger thrust and a smaller thrust ripple than the other [9].

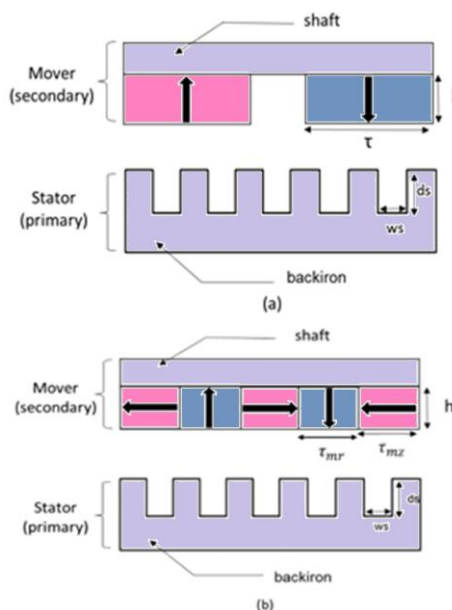


Figure 5: PMLSM topologies. (a) Radial array, (b) Quasi-Halbach array.

### 6. FLUX DENSITY AND THRUST FORCE COMPARISON OF RADIAL AND HALBACH ARRAY PMLSM

As mentioned before, the design of the motor becomes complicated due to complex geometry and material saturation.

The reluctance variation of the motor has an important role on the performance; hence, an accurate knowledge of the flux distribution inside the motor for different excitation currents and rotor positions is essential for the prediction of the motor performance.

To predict PMLSM behavior in each configuration, analysis of the magnetic flux is an essential part of design procedure. So, flux waveforms in all parts of the machine should be calculated. As FEM is well-known method for field solution and design validation of motors; it is used as efficient tool for accurate evaluation of the motor performance in the proposed configuration.

The Halbach topology has a self-shielding property and higher flux density than radial topology. Also, the back-iron of Halbach topology does not saturate after optimization.

The lines and value of the flux density for radial array and Halbach array topologies are shown in Figure 6.

The obtained results from FEM analysis such as flux density and trust force in the two structures are compared. Figure 7 shows the simulated flux density of Halbach and radial array topologies.

The results of trust force for radial array and Halbach array topologies are shown in Figure 8. It is seen that trust force increases effectively in a PMLSM with Halbach array.

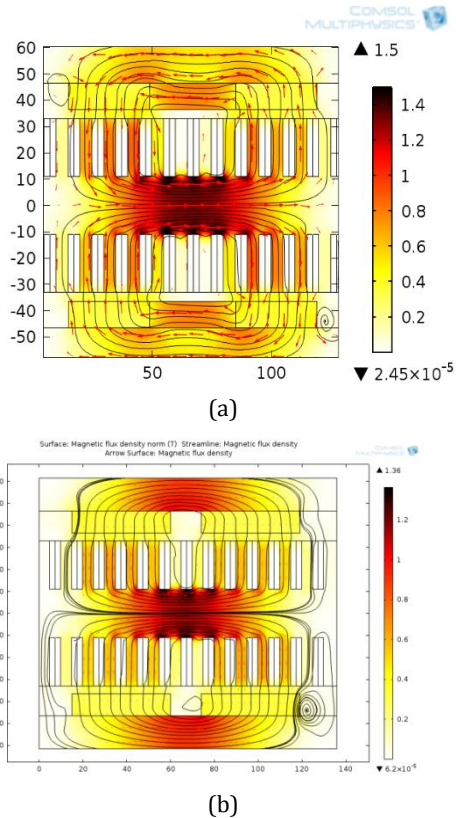


Figure 6: Flux distributions in PMLSM. (a) Radial array, (b) Halbach array.

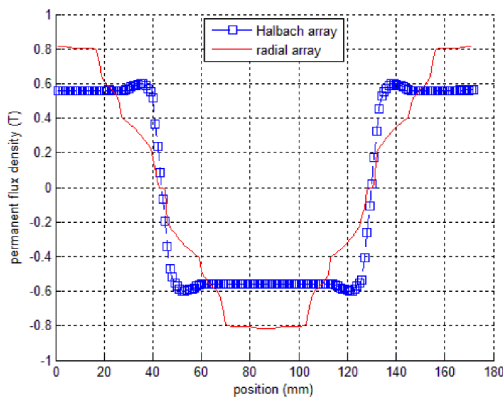


Figure 7: Comparison flux density of Halbach and radial array topologies.

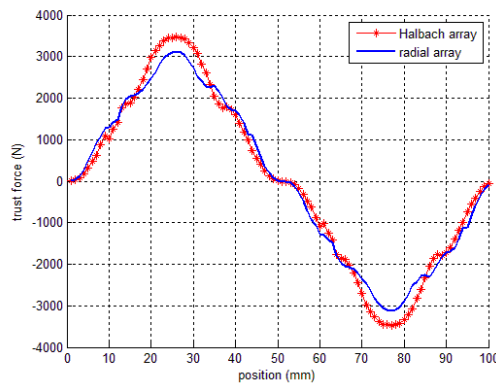


Figure 8: Thrust force of Radial array and Halbach array Topologies.

### 7. DESIGN OPTIMIZATION OF EMALS BASED ON 2-D FEM ANALYSIS

In this paper, the objective function is maximization of the average thrust. This improvement may cause an increase in the amount of the permanent magnet which leads to an increase in the cost of the motor. The constraints are maximum flux density in teeth ( $B_{max}$ ) and maximum current flow ( $i_{max}$ ). The parameters affecting thrust force are chosen as design variables and the other parameters are selected as fixed variables. The design variables and constraints are listed in Table 1.

TABLE 1  
NOMINAL VALUE OF THE GEOMETRICAL PARAMETERS OF THE PMLSM.

	Symbol	Constraints	Unit
Magnet width	$C_{wm}$	34-70	mm
Magnet thickness	$C_{wm}$	10-7	mm
Coil diameter	$C_{ds}$	7-11	mm
Slot depth	$C_{dc}$	19-25	cm
Slot width	$C_{ws}$	40-55	mm

Table 2 shows the amplitudes of thrust of PMLSM obtained from FEM analysis under different width of the vertical magnetized magnet. The design variables are divided to five values for full range. The results indicate that the thrust increases as the width of the PM is increased, but the increasing rate slows down and tends to saturate. The highest amplitude of the thrust of PMLSM is obtained for the Width of PM=63 mm. Table 3 shows the amplitudes of thrust of PMLSM obtained from 2-D FEM analysis under different thickness of the PM. The results indicate that the thrust increases as the thickness of the PM increases. The maximum thrust of PMLSM is 12420 N for the thickness of PM=16 mm. The analysis of the effect of the coil diameter is very important for estimating the actual performance. The responses of the thrust amplitudes under different coil diameters are shown in table 4. The thrust amplitude increases according to the increase of the coil diameter, but the latter is limited by current constraint. The maximum thrust is 12470 N for the coil diameter=10 mm.

TABLE 2  
THE AMPLITUDE OF THRUST OF PMLSM OBTAINED BY 2-D FEM ANALYSIS UNDER DIFFERENT PM WIDTH.

Width of PM (mm)	Maximum Thrust ( $10^4$ N)
34	1.205
43	1.214
52	1.227
63	1.251
70	1.238

The higher thrust amplitude obtained for the Width of PM=63 mm

TABLE 3  
THE THRUST AMPLITUDE RESULTS OBTAINED BY 2-D FEM ANALYSIS UNDER DIFFERENT THICKNESS OF THE PM.

Thickness of PM (mm)	Maximum Thrust (104 N)
10	1.211
12	1.218
14	1.227
16	1.242
17	1.233

The maximum thrust of PMLSM is 12420 N for the thickness of PM=16 mm

TABLE 4  
THE AMPLITUDE OF THRUSTS OF PMLSM OBTAINED BY 2-D FEM ANALYSIS UNDER DIFFERENT COIL DIAMETER.

Coil diameter (mm)	Maximum Thrust (104 N)
7	1.225
8	1.234
9	1.238
10	1.247
11	1.241

The maximum thrust of PMLSM is 12470 N for the coil diameter=10 mm

TABLE 5  
THE AMPLITUDE OF THRUSTS OF PMLSM OBTAINED BY 2-D FEM ANALYSIS UNDER DIFFERENT SLOT DEPTH.

Slot depth (mm)	Maximum Thrust (104 N)
19	1.211
21	1.217
23	1.224
25	1.230

The maximum thrust of PMLSM is 12240 N for the slot depth =25 mm

Table 5 shows the thrust amplitude under different slot depth ( $C_{ds}$ ), obtained by 2-D FEM analysis.

The results indicate that the thrust increases as the slot depth increases, but its rate slows down and tends to saturate.

The highest amplitude of thrust of PMLSM is obtained for the slot depth =25 mm.

Table 6 shows the thrust amplitude under different width of slot.

The thrust is increased by increasing the width of slot, but the latter is limited by flux density constraint. The highest amplitude of thrust of PMLSM is obtained for the width of slot =56 mm.

TABLE 6  
THE THRUST AMPLITUDE UNDER DIFFERENT SLOT WIDTH OBTAINED BY 2-D FEM ANALYSIS.

Slot width (mm)	Maximum Thrust (10 <sup>4</sup> N)
38	1.250
43	1.258
51	1.265
56	1.270

The maximum thrust of PMLSM is 12700 N for the slot width =56 mm

Table 7 lists the values of optimized design variables and fixed variables. By design optimization, the thrust force is increased 12.84 N compared to the design without optimization.

TABLE 7  
THE VALUES OF OPTIMIZED DESIGN VARIABLES AND FIXED VARIABLES.

	Symbol	Value	Unit
Magnet width	$C_{wm}$	63	mm
Magnet thickness	$C_{hm}$	16	mm
Coil diameter	$C_{ds}$	10	mm
Slot depth	$C_{dc}$	25	cm
Slot width	$C_{ws}$	56	mm
Pole pitch	$\tau$	60	mm
Slot pitch	$\tau_s$	11	mm
Residual flux density	$B_r$	1.3	T
Air gap length	$g$	3.2	cm
Rated current	$I_m$	425	A

## 8. CONCLUSIONS

In this paper, a modest attempt has been done to compare two PM mover with quasi-Halbach array topology and radial topology for PMLSM application and design a double-sided PMLSM in EMALS. An analysis based on Maxwell equations has been done to predict air-gap magnetic flux density distribution. By using the finite element method, the effects of the parameters on the thrust amplitude for EMALS have been analyzed. The design optimization of quasi-Halbach array magnet configuration helps in achieving high thrust force and uniform flux density along the air gap of the PMLSM, as well as reducing thrust force ripple.

## REFERENCES

- [1] R.R. Bushway, "Electromagnetic aircraft launch system development considerations," *IEEE Trans. Magn*, vol. 37, no. 1, pp. 52-54, Jan. 2001.
- [2] M.R. Doyle, D.J. Samuel, T. Conway, and R. R. Klimowski, "Electromagnetic aircraft launch system-EMALS," *IEEE Trans. Magn*, vol. 31, no. 1, pp. 528 - 533, Jan. 1995.

- [3] D. Patterson, A. Monti, C.W. Brice, R.A. Dougal, R.O. Pettus, S. Dhulipala, D.C. Kovuri, and T. Bertonecelli, "Design and simulation of a permanent-magnet electromagnetic aircraft launcher," *IEEE Trans. Magn*, vol. 41, no. 2, pp. 566 - 575, March/April 2005.
- [4] H. Gör and E. Kurt, "Preliminary studies of a new permanent magnet generator (PMG) with the axial and radial flux morphology," *International Journal of Hydrogen Energy*, vol. 41, no. 17, pp. 7005-7018, 2016.
- [5] L. Chunyan, and K. Baoquan, "Research on electromagnetic force of large thrust force pmlsm used in space electromagnetic launcher," *IEEE Transactions on Plasma Science*, vol. 41, no. 2, pp. 1209 - 1213, 2013.
- [6] Sh. Jung-Seob, T. Koseki, and K. Houng-Joong. "Proposal and design of short armature core double-sided transverse flux type linear synchronous motor," *IEEE Trans. Magn*, vol. 48, no. 3, pp. 3871- 3874, 2012.
- [7] Ch.E. Kim, S.H. Lee, D.H. Lee, and H.J. Kim, "The analysis of permanent magnet double-sided linear synchronous motor with perpendicular arrangement," *IEEE Trans. Magn*, vol. 49, no. 5, pp. 2267 - 2270, 2013.
- [8] S.M. Jang, S.H. Lee, and I.K. Yoon, "Design criteria for detent force reduction of permanent-magnet linear synchronous motors with halbach array," *IEEE Trans. Magn*, vol. 38, no. 5, pp. 3261-3263, 2002.
- [9] K. Bao-Quan, W. Hong-Xing, L. Li-Yi, Zh. Liang-Liang, Zh. Zhe, and C. Hai-Chuan, "The thrust characteristics investigation of double-side plate permanent magnet linear synchronous motor for eml," *IEEE Trans. Magn*, vol. 45, no. 1, pp. 501-505, 2009.
- [10] S. M. Jang and S. H. Lee, "Comparison of two types of PM linear synchronous servo and miniature alternator with air-cored film coil," *IEEE Trans. Magn*, vol. 38, no. 5, pp. 3264-3266, 2002.
- [11] K. Ng, ZQ.Zhu, and D. Howe. "Open-circuit field distribution in a brushless motor with diametrically magnetized pm motor, accounting for slotting and eddy current effects," *IEEE Trans. Magn*, vol. 32, no. 5, pp. 5070-5072, 1996.
- [12] S. Kül, O. Bilgin, and M. Mutluer, "Application of finite element method to determine the performances of the line start permanent magnet synchronous motor," *Procedia - Social and Behavioral Sciences*, vol. 195, pp. 2586-2591, 2015.

#### BIOGRAPHIES



**Hassan Moradi Cheshmeh Beigi** received his M.Sc. in 2005 and Ph.D. in 2010, both in Power Elec. Eng. from Shahid Beheshti University, Tehran, Iran. He is now a faculty member of Electrical Engineering Department of Razi University, Kermanshah Iran. His research interests are include: Novel electric machines for different applications, Electrical motor design, Power converters for electric machines.

**Allahdad Khanmohamadian** received his M.Sc. degree in Electrical Engineering from the University of Razi, Kermanshah, Iran, in 2016. His research interest is Power converter for electrical machines.

#### How to cite this paper:

H. Moradi Cheshmeh Beigi and A. Khanmohamadian, "Comparison of radial and halbach array PMLSM by employing 2-D electromagnetic finite element analysis," *Journal of Electrical and Computer Engineering Innovations*, vol. 4. no. 2, pp. 111-117, 2016.

**DOI:** 10.22061/jecei.2016.571

**URL:** [http://jecei.srttu.edu/article\\_571.html](http://jecei.srttu.edu/article_571.html)

